NREL
NATIONAL RENEWABLE ENERGY LABORATORY

Test Cases for Wind Power Plant Dynamic Models on Real-Time Digital Simulator

Preprint

M. Singh, E. Muljadi, and V. Gevorgian

To be presented at the IEEE Symposium on Power Electronics and Machines in Wind Applications
Denver, Colorado
July 16–18, 2012

Conference Paper
NREL/CP-5500-55314
June 2012

Contract No. DE-AC36-08GO28308

Available electronically at http://www.osti.gov/bridge

Available for a processing fee to U.S. Department of Energy
and its contractors, in paper, from:

U.S. Department of Energy
Office of Scientific and Technical Information
P.O. Box 62
Oak Ridge, TN 37831-0062
phone: 865.576.8401
fax: 865.576.5728
email: mailto:reports@adonis.osti.gov

Available for sale to the public, in paper, from:

U.S. Department of Commerce
National Technical Information Service
5285 Port Royal Road
Springfield, VA 22161
phone: 800.553.6847
fax: 703.605.6900
email: orders@ntis.fedworld.gov
online ordering: http://www.ntis.gov/help/ordermethods.aspx

Cover Photos: (left to right) PIX 16416, PIX 17423, PIX 16560, PIX 17613, PIX 17436, PIX 17721

Printed on paper containing at least 50% wastepaper, including 10% post consumer waste.

Test Cases for Wind Power Plant Dynamic Models on Real-Time Digital Simulator

M .Singh, E. Muljadi, V. Gevorgian

***Abstract*-- The objective of this paper is to present test cases for wind turbine generator and wind power plant models commonly used during commissioning of wind power plants to ensure grid integration compatibility. In this paper, different types of wind power plant models based on the Western Electricity Coordinating Council Wind Generator Modeling Group's standardization efforts are implemented on a real-time digital simulator, and different test cases are used to gauge their grid integration capability. The low-voltage ride through and reactive power support capability and limitations of wind turbine generators under different grid conditions are explored. Several types of transient events (e.g., symmetrical and unsymmetrical faults, frequency dips) are included in the test cases. The differences in responses from different types of wind turbine are discussed in detail.**

***Index Terms*—Wind power generation, real-time digital simulator, LVRT**

I. Introduction

THIS paper describes results from implementation of the standard Western Electricity Coordinating Council (WECC) aggregate wind power plant (WPP) models on a real-time digital simulator (RTDS). The RTDS hardware platform allows solving of time-domain bulk power system models in real time, and the wind power plant models described here are intended to be integrated into these bulk power system models. The use of RTDS also brings an additional advantage: Hardware-in-the-loop testing of turbines, controls, and protection can also be performed in the future.

So far, real-time modeling efforts for wind power have concentrated on detailed modeling of individual turbines [1, 2, 3]. Each of these turbines is a generator, and each usually has a power converter that employs switches operating at kilohertz switching frequencies and requires very small time steps for simulation. For use in bulk power system simulations, individual turbine models can be very computationally expensive because regions typically contain numerous wind power plants with up to hundreds of turbines each. For the RTDS platform, the number of devices being modeled correlates strongly with the amount of simulation hardware required. Hence, computationally expensive models translate to monetary expense. In this situation, to enable simulation of large power networks on the RTDS, we propose the use of aggregate wind power plant models. These models have been developed for the PSLF and PSS/E software platforms by the WECC Wind Generator Modeling Group and have been validated against real data [4, 5]. There are four standard models based on distinctions in electrical generator and converter topology, and these models and their implementation are discussed in the next section. Section III describes the results from the RTDS simulations. The results here are similar to the results obtained using other software as described in our prior work on short-circuit behavior of wind power plants [6, 7].

M. Singh, E. Muljadi, and V. Gevorgian are with National Renewable Energy Laboratory, Golden, CO, USA (e-mail: eduard.muljadi@nrel.gov).

II. WECC Wind Power Plant Models

A. Types of Wind Power Plants

Detailed description of the WECC model development has been provided in [4]. The difference among the turbine types is mostly based on the electrical generation part (generator, power converter, and the control algorithm used). The control strategies used to control the prime mover are generally similar across turbine types. They commonly use mechanical brakes and blade pitch control to avoid runaway condition and keep the mechanical stresses on the mechanical components of the wind turbine generator (WTG) within the operating range of the design tolerance.

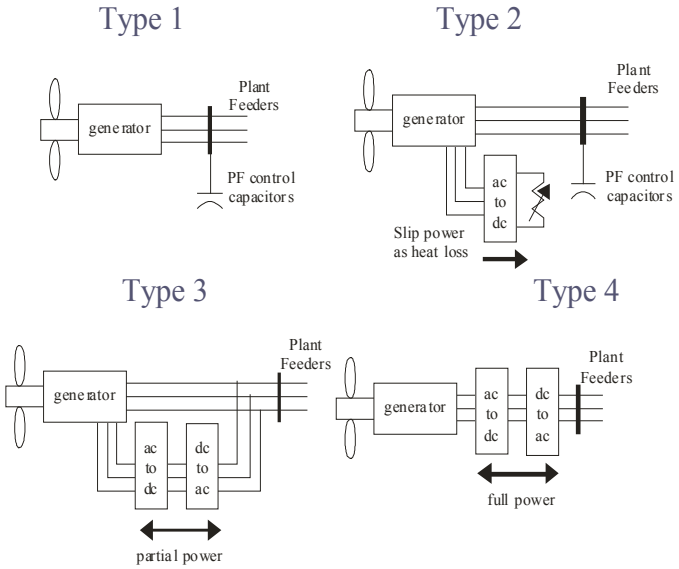

Fig. 1. Wind turbine types classified by generator and converter topology

The pitch angle of the blades is usually controlled in the high wind speed region to keep the aerodynamic power within

limits. Thus, the output power and/or rotor speed can be kept within its boundary limits.

Figure 1 shows the different turbine types. Type 1 generators have only pitch control to regulate average aerodynamic power above rated wind speeds and avoid runaway problems during loss of line connection. The output power is not regulated, and it will vary with the operating slips. In Type 2 generators, there is pitch control to regulate average aerodynamic power above rated wind speeds and to avoid runaway problems. The output power is regulated by an external rotor resistance controller to maintain the rated output power of the generator when the wind speed is above rated winds. In Type 3 generators, a wound rotor induction generator with partial-size power converter is connected to the rotor winding. There is a pitch control to regulate average aerodynamic power above rated wind speeds and avoid runaway problems. The output power is regulated by the power converter to maintain optimum aerodynamic efficiency of the wind turbine by operating in a variable-speed operation. Type 4 generators employ a wind turbine with a full-rating power converter connecting the grid to the generator. There is pitch control to regulate average aerodynamic power above rated wind speeds and avoid runaway problems. The output power is regulated by the power converter to maintain optimum aerodynamic efficiency of the wind turbine by operating in a variable-speed operation.

B. One-Line Representation of Wind Power Plants

For bulk system studies, it is impractical and unnecessary to model the collector system network inside the plant to the level of detail shown in Figure 2.

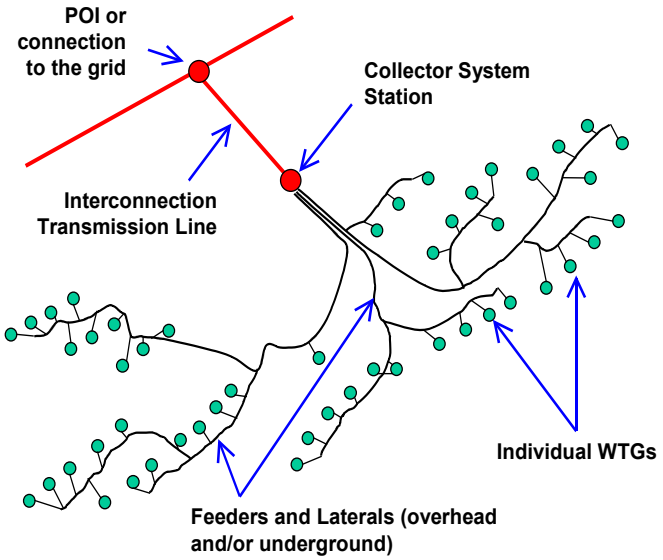

Fig. 2. Physical layout of a wind power plant

The single-machine equivalent model shown in Figure 3 is the recommended approach to represent WPPs in WECC base cases [4]. For the vast majority of WPPs, regardless of size or configuration, a single generator equivalent is sufficient for planning studies. In some situations where there are two or more types of WTGs in the plant, or when the plant contains feeders with very dissimilar impedance, the plant may be represented with two equivalent generators. This representation has been shown to be sufficient for bulk-level dynamic simulations.

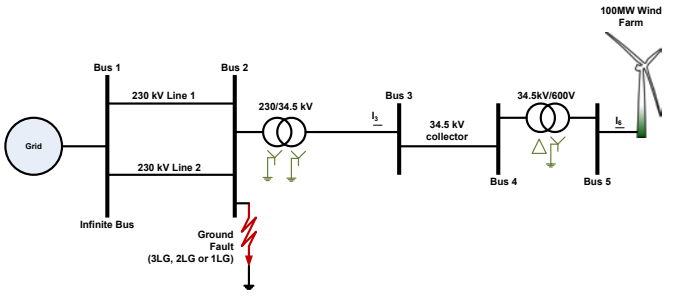

Fig. 3. One-line representation of a WPP, including single-machine equivalent model

C. Voltage and Reactive Power Control

The WECC models incorporate reactive power controls. In general, WTG Type 1 and WTG Type 2 have switched-bank capacitors to regulate the reactive power at the turbine level such that the output power factor of individual turbines will be unity as the size of capacitors is varied with the wind speed. WTG Type 3 and Type 4 have the ability to control the reactive power and real power instantaneously and independently via their power converters. Thus, the reactive power can be controlled at a constant value or can be controlled to regulate the voltage at the terminal or a remote bus, or it can be controlled to maintain a specific power factor. At the WPP level, reactive power compensation may be needed at the point of interconnection (POI). (Usually, it is installed at the low-voltage side.) The plant-level reactive power can be implemented by static capacitors, static compensators, or STATCOM.

D. Low Voltage Ride-Through Capability

In the future, more WTGs and other renewable energy sources will be connected to the grid. A large number of conventional power plants will be replaced by renewable energy sources—especially in rich-resource areas. As the size of the WPP increases, the reliability and availability of the WPP must be improved so it will stay connected during and after transient events. The transient events most likely occur in the power system network outside the WPP. The WPP should be immune to disturbances and designed to have ride-through capability so that transient events will not disconnect it from the grid and to keep the balance of generation and load in the power system. Any large imbalance of power in the power system network may lead to frequency variations and under- and over-voltage conditions, and eventually the relay protection may trigger disconnection of generators from the grid and cause a cascading effect or worse (blackout). The WECC models incorporate low-voltage ride through (LVRT)

characteristics, and this capability has been demonstrated in the Type 3 turbine results.

III. Simulation Results From Real-Time Digital Simulator

A. Type 1 Wind Power Plant Results

Once the WECC models were implemented in RSCAD/RTDS, we tested the ability of the models to show dynamic behavior of the Type 1 turbine under fault (under both balanced and unbalanced fault conditions). The turbine model in RSCAD was set to run at full output power (1 pu). A nine-cycle (150 ms) fault (3LG balanced and SLG on Phase A) was applied at the POI once the model reached steady state. The results for the 3LG fault are shown in Figure 4. The SLG fault results are shown in Figure 5. Note that dynamics in power and speed persist long after the fault has cleared because of mechanical inertia.

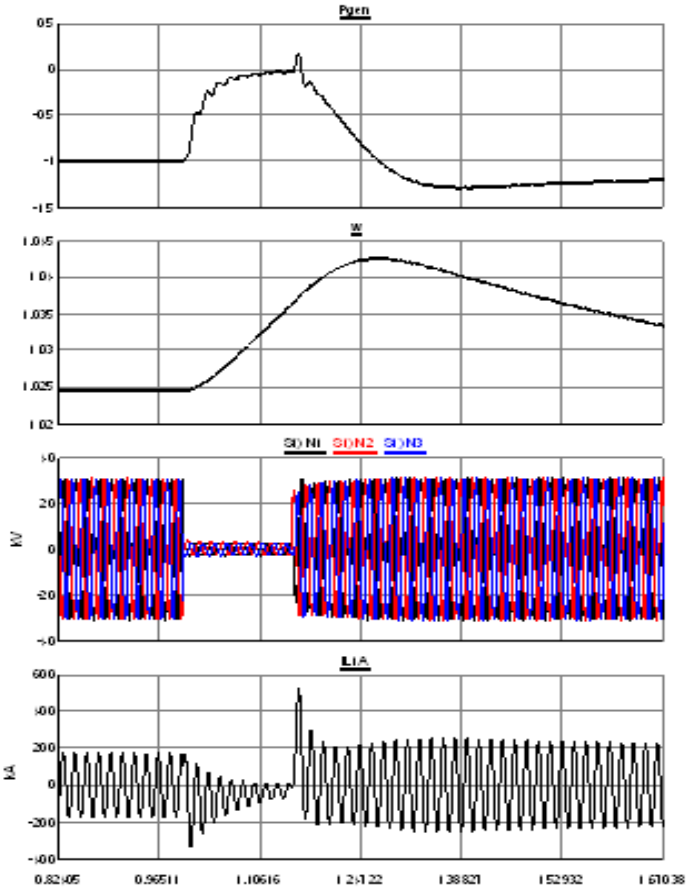

Fig. 4. Power in pu (top), speed in pu (second from top), three-phase voltage at POI in kV (second from bottom), and Phase A current (bottom) for a 3LG fault on a Type 1 machine

In Figure 4 (3LG fault), in the prefault stage, the plant is operating at full power output (-1 pu, where the negative sign denotes that power is flowing out of the plant) and at approximately 1.025 pu speed. In the case of a 3LG fault, the voltage sags to near 0, and the power output plummets to 0 and then recovers once the fault clears. Note that the LVRT characteristic is not in place here, and even if it was, the plant would still be expected to ride through for a fault of this duration. Currents are measured at the pad-mounted transformer secondary (plant side), and the expected transients at fault inception and clearing are visible.

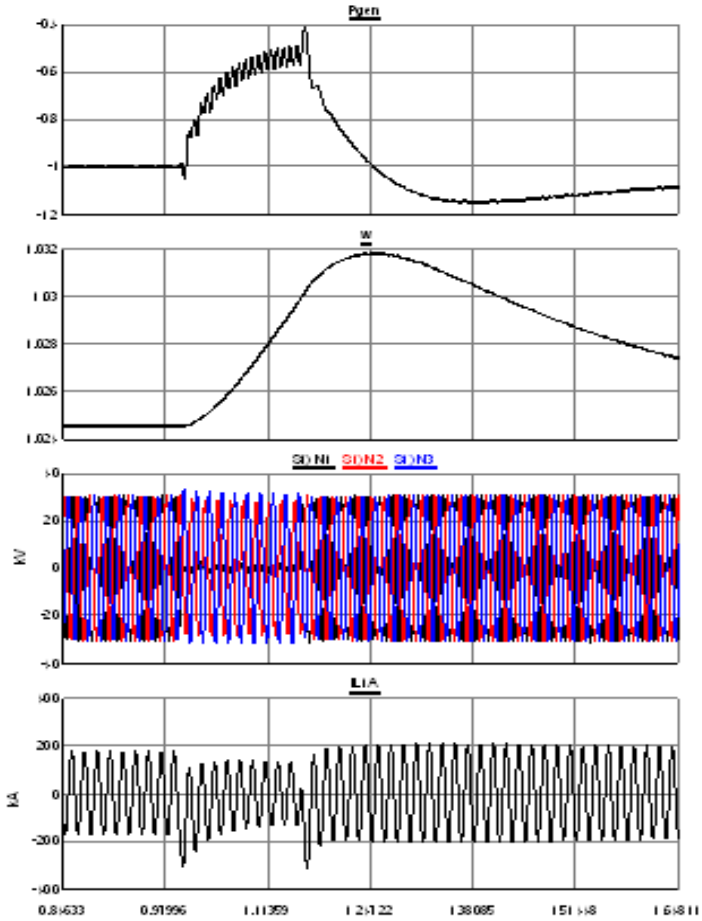

Fig. 5. Power in pu (top), speed in pu (second from top), three-phase voltage at POI in kV (second from bottom), and Phase A current (bottom) for an SLG fault on a Type 1 machine

Figure 5 (SLG fault) shows the effects of an unbalanced event. This analysis would not be possible using the WECC models in PSLF or PSS/E and requires time-domain models. In the voltage plot (second from bottom), Phase A voltage drops to near 0, and the other two phases change only slightly in magnitude. Real power output drops but not to the extent seen in Figure 4 for the 3LG fault. Results for LL and LLG faults have also been obtained but have been omitted from this paper for the sake of brevity.

Figure 6 shows another demonstration of the model capabilities. For this test, a frequency step change from 60 Hz to 59.5 Hz was simulated (see bottom plot), and the model's response was observed. The model does provide inertial response, as when the frequency drops, the plant power output jumps (see top plot) as generator speed decreases (second from top). This indicates that kinetic energy stored in the rotors of the plant's turbines is being extracted and delivered to the grid. There is a corresponding increase in line current, as expected (see second-from-bottom plot). The plant settles at a new speed that allows it to deliver rated power at this new frequency. This frequency test has been conducted for

generators of all types, though the plots for types 2, 3, and 4 have not been included for the sake of brevity. From the plots, it was seen that Type 1 turbines provided the most inertial response and Type 4 turbines the least.

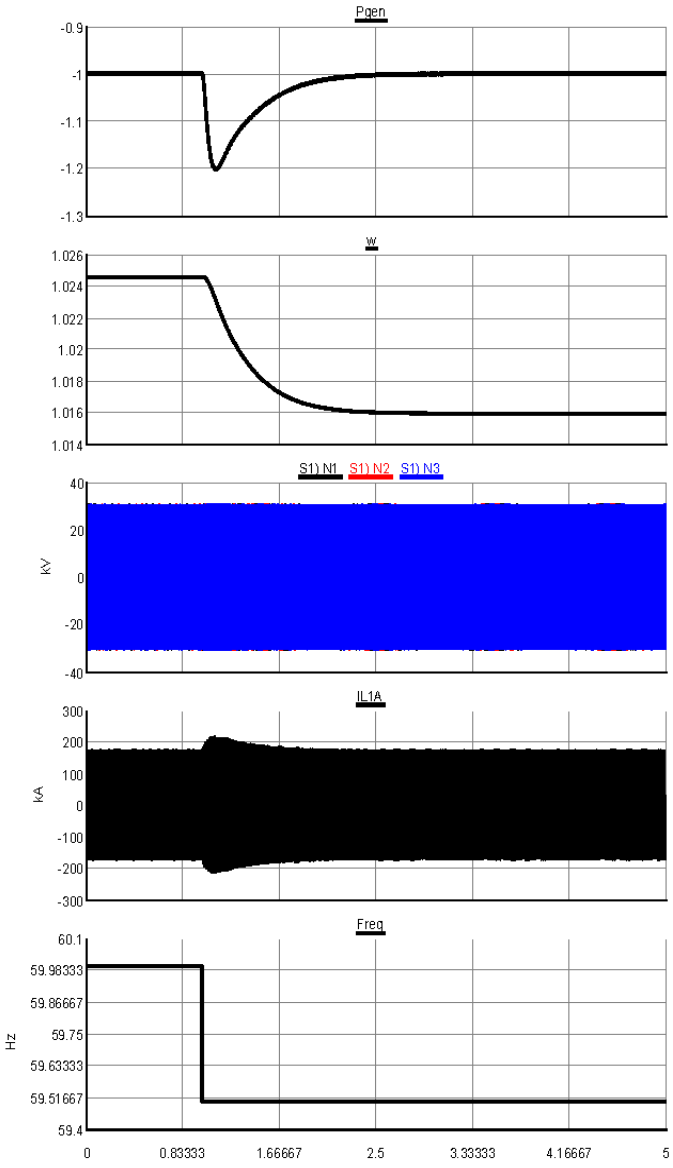

Fig. 6. Power in pu (top), speed in pu (second from top), three-phase voltage at POI in kV (third from top), Phase A current (second from bottom), and system frequency (bottom) for Type 1 machine

B. Type 2 Wind Power Plant Results

The dynamics of Type 2 machines differ considerably from those of Type 1 machines because of the presence of a controllable external rotor resistance. This resistance works in conjunction with the pitch control to reduce the stress on the turbine through control of speed. The results from the application of a 3LG fault on a Type 2 machine are shown in Figure 7. As in the Type 1 case, at the prefault stage, the plant is operating at full power output (-1 pu, where the negative sign denotes that power is flowing out of the plant) and at approximately 1.025 pu speed. In the case of a 3LG fault, power output plummets to 0 and then recovers once the fault clears, while speed rises briefly. Resistance change is negligible during the fault, but a small rotor resistance change can be seen during the recovery time after the fault due to the speed change.

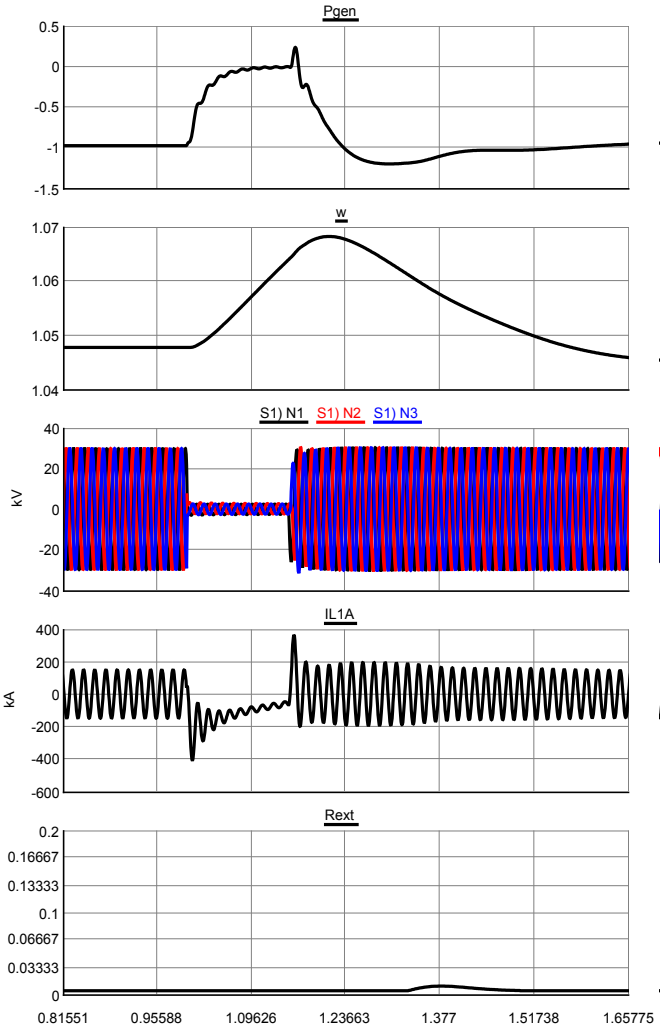

Fig. 7. Power in pu (top), speed in pu (second from top), three-phase voltage at POI in kV (second from bottom), and Phase A current (bottom) for a 3LG fault on a Type 2 machine

Figure 8 (SLG fault) shows the effects of an unbalanced event. Once again, it should be noted that this analysis would not be possible using the WECC models in PSLF or PSS/E; it requires time-domain models. In the voltage plot (second from bottom), Phase A voltage drops to near 0, and the other two phases change only slightly in magnitude. Real power output drops, but not to the extent seen in Figure 7 for the 3LG fault. In this case, the external rotor resistance does not activate at all because the fault does not cause a sufficient speed change for the resistance controller to respond. Results for LL and LLG faults have also been obtained but have been omitted from this paper for the sake of brevity.

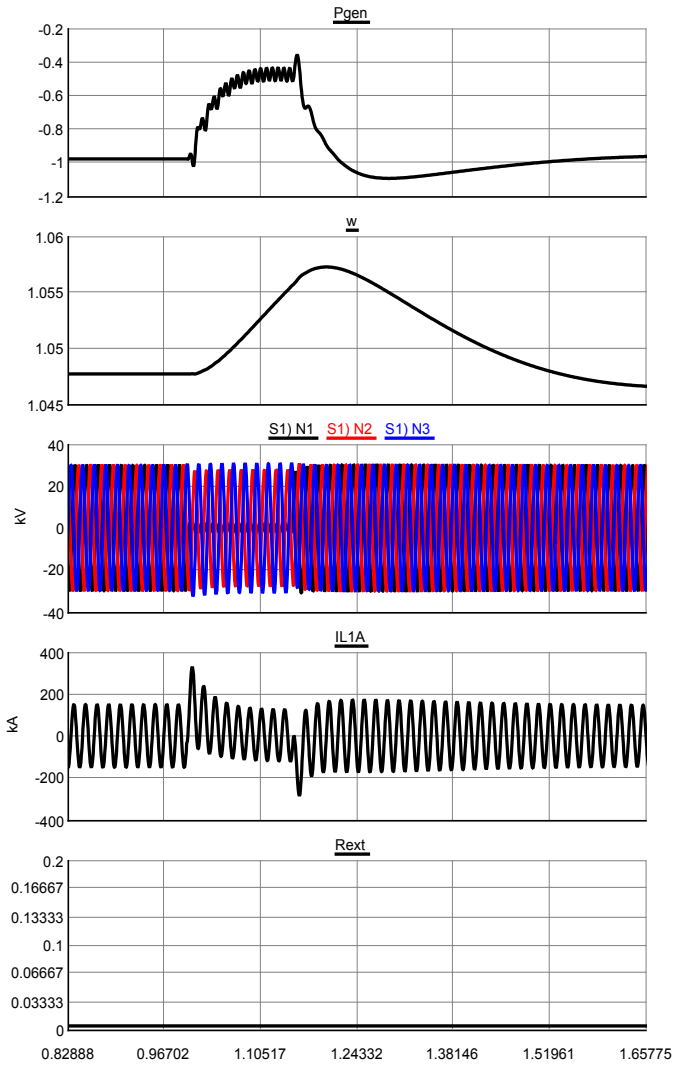

Fig. 8. Power in pu (top), speed in pu (second from top), three-phase voltage at POI in kV (second from bottom), and Phase A current (bottom) for an SLG fault on a Type 2 machine

C. Type 3 Wind Power Plant Results

For testing of Type 3 models, a different strategy must be adopted. The WECC model uses an equivalent current source representation for doubly-fed induction generator (DFIG) plants, and this representation does not allow for testing of unbalanced events because the output of the current source is always positive-sequence only, while the output of a real plant may include a negative-sequence component [7]. However, there are still many tests that can be performed using this model in RTDS. Figure 9 shows a nine-cycle three-phase fault at the POI. This fault is not as severe as the ones depicted in the Type 1 and Type 2 cases to prevent the LVRT logic from kicking in and results in a voltage drop from 1 pu to 0.8 pu. In this case, in the prefault stage, the plant is operating at rated power output (200 MW) (note that this is output power in MW and not in pu as in previous cases) and delivering 0 MVAR of reactive power. In the case of a 3LG fault, power output initially drops, stabilizes, and then recovers once the fault clears. Currents are measured at the transformer secondary side (plant side), and the expected transients at fault inception and clearing are visible. It should be noted that the reactive power also changes in a similar fashion. Also note the decoupling of real and reactive power. The converter is capable of riding through a voltage drop of this magnitude without the LVRT logic being required. Machine speed barely changes at all from its set point of 1.2 p.u. during the fault event. Transients aside, the Type 3 model shows remarkably stable behavior during this fault event.

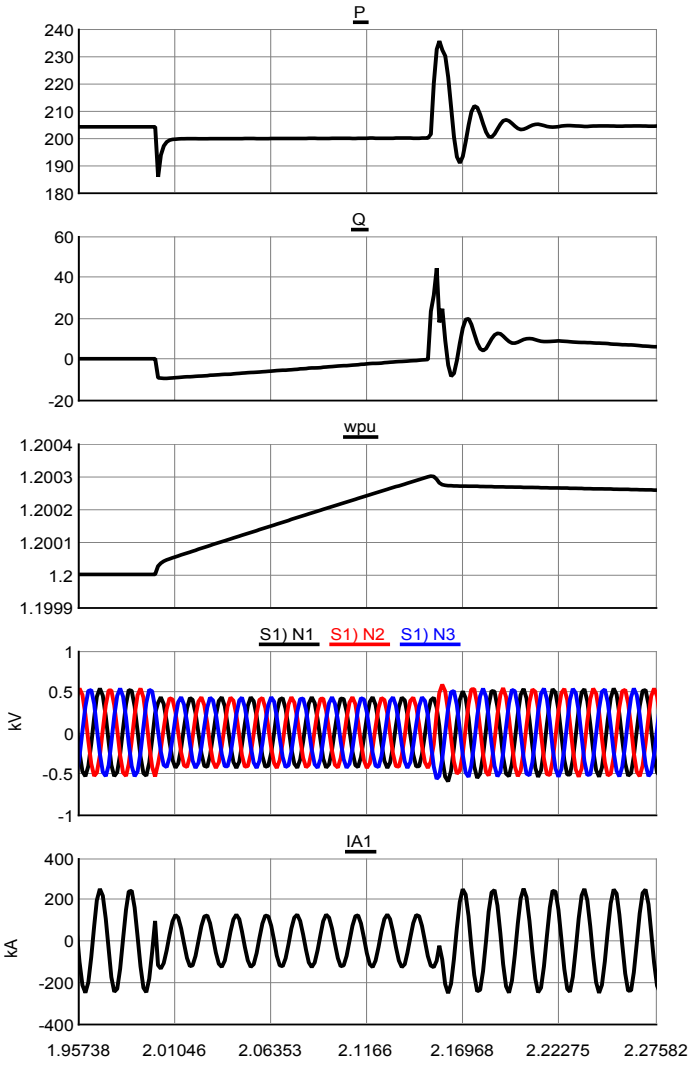

Fig. 9. Power in MW (top), reactive power in MVAR (second from top), speed in pu (third from top), three-phase voltage at POI in kV (second from bottom), and Phase A current (bottom) for a 3LG fault on a Type 3 machine

Figures 9 and 10 show the LVRT logic acting in the case of a severe three-phase fault. The LVRT characteristic used here is based on GE's zero-voltage ride through characteristic [4]. As soon as the RMS voltage at the POI drops below 0.9 pu, the LVRT logic triggers. From then on, at each instant, the actual voltage is compared with the characteristic's upper and lower voltage limits, which change with time. If the voltage leaves the characteristic envelope, a latching trip signal transitions from 0 to 1 and results in a breaker tripping the plant offline. In Figure 10, a nine-cycle event is shown in which the severe three-phase fault causes the voltage at the POI to drop to 0 for

nine cycles. However, the voltage recovers and never leaves the LVRT envelope, and hence, no trip signal is issued. In Figure 11, a 15-cycle event is shown, and in this case, the voltage drops to 0 for 15 cycles. This causes the actual voltage to fall below the lower limit of the LVRT characteristic, and the actual voltage thus briefly leaves the LVRT envelope. In this case, a trip signal is immediately issued.

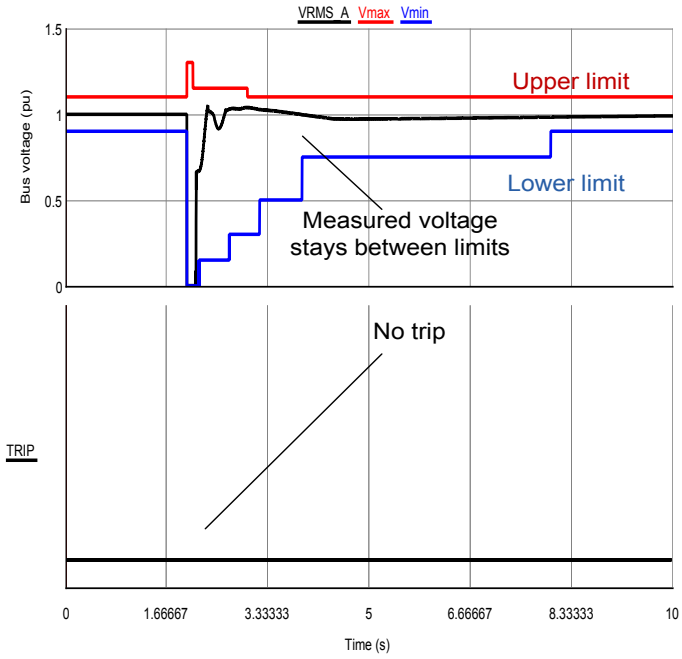

Fig. 10. RMS voltage in pu, with time-dependent LVRT upper and lower voltage limits (top) and status of trip signal (bottom) for a severe nine-cycle three-phase fault

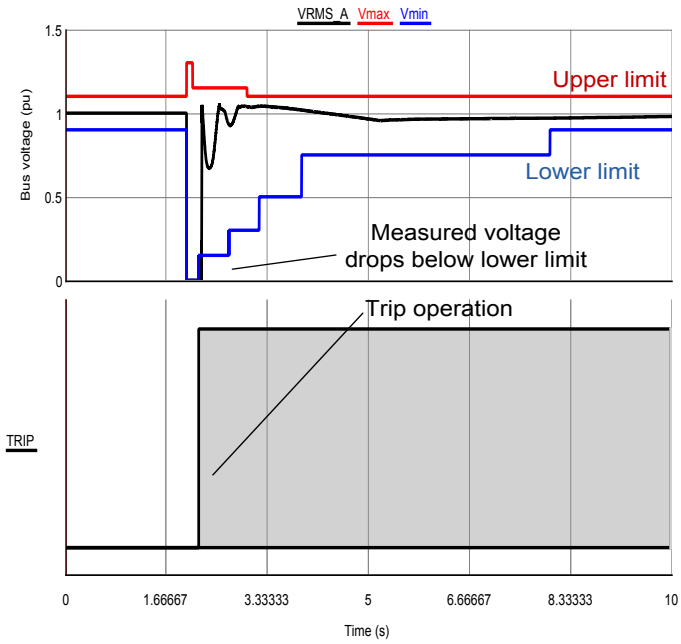

Fig. 11. RMS voltage in pu, with time-dependent LVRT upper and lower voltage limits (top) and status of trip signal (bottom) for a severe 15-cycle three-phase fault

D. Type 4 Wind Power Plant Results

For Type 4 WPP models, once again the WECC model employs an equivalent current source representation. The Type 4 model has no mechanical state variables at all. The response of the Type 4 model is broadly similar to the Type 3 turbine response but with a few critical differences. In Figure 12, in the prefault stage, the plant is operating at rated power output (200 MW) and delivering -10 MVAR of reactive power. In the case of a 3LG fault, aside from transients at the start and end of the event, the power output remains totally flat. Currents are measured at the transformer secondary side (plant side), and the expected transients at fault inception and clearing are visible. It should be noted that the reactive power also barely changes. This flat response is due to the entire output of the plant having to pass through the power converters. The factor limiting the response is the converter current limit, which protects the switches in the individual converters. This limit may typically range from 1.1 pu to 1.5 pu of the rated current. The WECC Type 4 model incorporates a current limit logic that changes the converter behavior during faults [4].

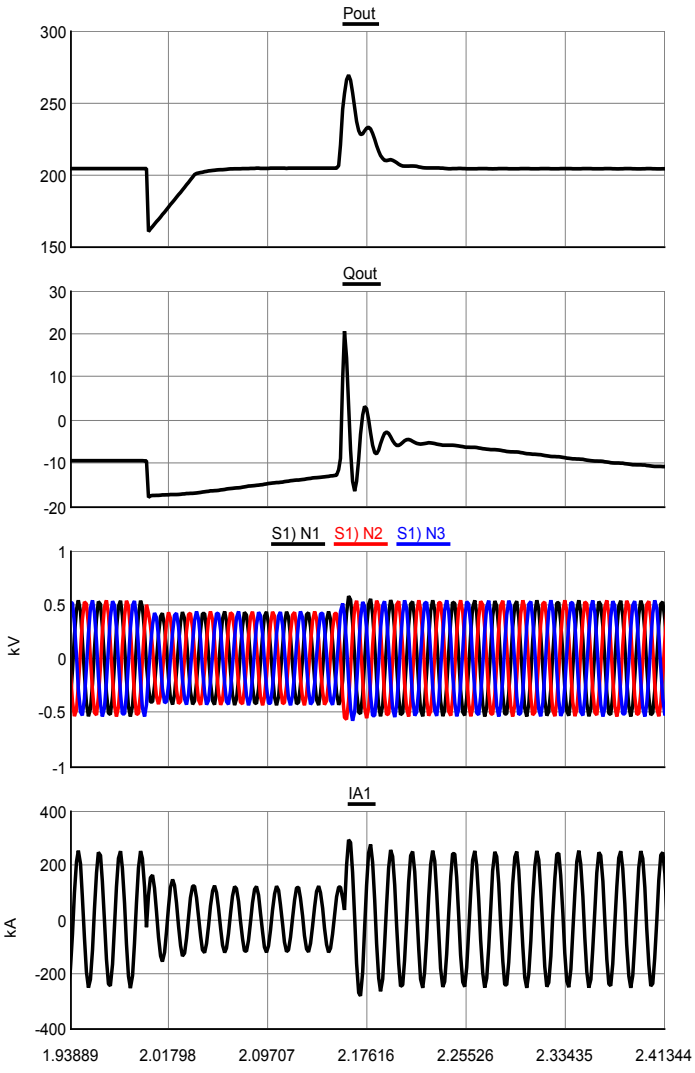

Fig. 12. Power in MW (top), reactive power in MVAR (second from top), three-phase voltage at POI in kV (second from bottom), and Phase A current (bottom) for a 3LG fault on a Type 4 machine

IV. Conclusion

In summary, the results of RTDS simulations of four types of WPPs have been shown. The difference in response across WPP types has been explored. For Type 1 and Type 2 turbines, response to balanced and unbalanced faults has been examined, and for Type 3 and Type 4 turbines, balanced faults and LVRT have been examined. Inertial response has also been examined for all types of turbines. (Type 1 response has been shown as an example.) These models are aggregate models of WPPs that retain enough fidelity to reproduce the dynamics of WPPs. These models can be incorporated into bulk power system models for large geographical regions built on the RTDS, where using single turbine models for each of the hundreds of turbines within the region would be infeasible or impractical.

V. Acknowledgment

The authors gratefully acknowledge the support of RTDS Technologies and Nayak Corporation. This work was supported by the U.S. Department of Energy under Contract No. DE-AC36-08-GO28308 with the National Renewable Energy Laboratory.

VI. References

[1] Hui Li; Steurer, M.; Shi, K.L.; Woodruff, S.; Da Zhang , "Development of a Unified Design, Test, and Research Platform for Wind Energy Systems Based on Hardware-in-the-Loop Real-Time Simulation," *Industrial Electronics, IEEE Transactions on* , vol.53, no.4, pp.1144–1151, June 2006.

[2] Dae-Jin Park; Young-Ju Kim; Ali, M.H.; Minwon Park; In-Keun Yu , "A novel real time simulation method for grid-connected wind generator system by using RTDS," *Electrical Machines and Systems, 2007. ICEMS. International Conference on* , vol., no., pp.1936–1941, 8–11 Oct. 2007.

[3] Gagnon, R.; Sybille, G.; Bernard, S.; , D.; Casoria, S.; Larose, C. , "Modeling and real-time simulation of a doubly-fed induction generator driven by a wind turbine," IPST'05, June 2005.

[4] Muljadi, E.; Ellis, A., "Final project report-WECC wind generator development," March 2010.

[5] Behnke, M.; Ellis, A.; Kazachkov, Y.; McCoy, T.; Muljadi, E.; Price, W.; Sanchez-Gasca, J. , "Development and Validation of WECC Variable Speed Wind Turbine Dynamic Models for Grid Integration Studies," Proc. WINDPOWER 2007 Conference & Exhibition, Los Angeles, CA, June 24–28, 2007.

[6] Muljadi, E.; Samaan, N.; Gevorgian, V.; Jun Li; Pasupulati, S., "Short circuit current contribution for different wind turbine generator types," *Power and Energy Society General Meeting, 2010 IEEE* , vol., no., pp.1–8, 25–29 July 2010.

[7] Gevorgian, V.; Muljadi, E.; Singh, M., "Symmetrical and Unsymmetrical Fault Currents of a Wind Power Plant," *Power and Energy Society General Meeting, 2012 IEEE* , July 2012.

VII. Biographies

Mohit Singh (M'2011) received his M.S. and Ph.D. in Electrical Engineering from the University of Texas, Austin, in 2007 and 2011 respectively. His research is focused on dynamic modeling of wind turbine generators. Dr. Singh is currently working at the National Renewable Energy Laboratory in Golden, Colorado, USA, as a post-doctoral researcher in transmission and grid integration of renewable energy. His current interests include modeling and testing of various applications of wind turbine generators and other renewable energy resources. He is a member of the IEEE. He is involved in the activities of the IEEE Power and Energy Society.

Eduard Muljadi (M'82-SM'94-F'10) received his Ph. D. (in Electrical Engineering) from the University of Wisconsin, Madison. From 1988 to 1992, he taught at California State University, Fresno, California. In June 1992, he joined the National Renewable Energy Laboratory in Golden, Colorado. His current research interests are in the fields of electric machines, power electronics, and power systems in general with emphasis on renewable energy applications. He is member of Eta Kappa Nu and Sigma Xi and a Fellow of the IEEE. He is involved in the activities of the IEEE Industry Application Society, Power Electronics Society, and Power and Energy Society. He is currently a member of various committees of the IAS and a member of Working Group on Renewable Technologies and Dynamic Performance Wind Generation Task Force of the PES. He holds two patents in power conversion for renewable energy.

Vahan Gevorgian (M'97) graduated from the Yerevan Polytechnic Institute (Armenia) in 1986. During his studies, he concentrated on electrical machines. His thesis research dealt with doubly-fed induction generators for standalone power systems. He obtained his Ph.D. in Electrical Engineering from the State Engineering University of Armenia in 1993. His dissertation was devoted to a modeling of electrical transients in large wind turbine generators.

Dr. Gevorgian is currently working at the National Wind Technology Center of the National Renewable Energy Laboratory in Golden, Colorado, USA, as a research engineer. His current interests include modeling and testing of various applications of small wind turbine-based power systems.